

Total energy, lattice dynamics, and structural phase transitions in silicon by the orthogonalized linear combination of atomic orbitals method

F. Zandiehnam

*Department of Physics and Astronomy, University of Kansas, Lawrence, Kansas 66045
and Department of Physics, University of Missouri—Kansas City, Kansas City, Missouri 64110-2499*

W. Y. Ching

Department of Physics, University of Missouri—Kansas City, Kansas City, Missouri 64110-2499

(Received 16 January 1990; revised manuscript received 1 March 1990)

We demonstrate the accuracy of the self-consistent orthogonalized linear combination of atomic orbitals method within the local-density approximation by applying it to ten different phases of Si. The electronic properties, total energies, and possible structural phase transitions are studied. Also calculated are the static properties of the diamond-structure Si including the equilibrium lattice constant, bulk modulus, and the pressure derivative of the bulk modulus along with the lattice dynamical properties of a few selective phonons at the zone-center Γ and the edge X points of the Brillouin zone. Furthermore, we have evaluated the internal strain parameter of the diamond-structure Si along the [111] direction. The results of our calculations are in very good agreement with the measured values and the results of the pseudopotential calculations.

I. INTRODUCTION

In recent years, accurate calculation of the total energy (TE) of simple crystals based on the Hohenberg-Kohn-Sham local-density-functional (LDF) theory¹ has become possible and extensively used to study the electronic and structural properties of materials. These properties include the equilibrium lattice constant, the bulk modulus, structural changes of bulk phases, cohesive energy, and even more complex problems associated with lattice vibrations, surfaces, interfaces, defects, etc. However, the accuracy of the total-energy calculation depends on the accuracy of the method of the electronic band calculation. Among the current methods, the pseudopotential,²⁻⁷ linear augmented-plane-wave (LAPW),⁸ linear muffin-tin orbitals (LMTO),⁹ and linear combination of atomic orbitals (LCAO) (Refs. 10-15) methods have been more extensively used and results in excellent agreement with the measured values have been obtained.

Several methods of band calculation have been applied to calculate the structural properties of Si by TE calculations. Si has been used as an excellent test case and is the most intensively studied solid. The most complete and accurate TE calculations on several phases of Si has been performed by Cohen *et al.*²⁻⁷ using the *ab initio* norm-conserving pseudopotential method (PM). They calculated the structural properties, such as the equilibrium volume (EV) and TE, bulk modulus, pressure derivative of the bulk modulus, pressure-induced phase transformations, lattice vibrational modes, and the electronic properties of several phases of Si. They obtained excellent results as compared with experiment. In the same series of calculations,⁵ they predicted several new high-pressure phases of Si, which included a hcp with two atoms in the unit cell, a fcc, a bcc, and a sc phase each with one atom

per primitive unit cell. Few years later, several independent experiments verified the hcp and fcc phase transformations.¹⁶⁻¹⁸ In 1988, Weyrich⁹ calculated the equilibrium bond length and the phonon frequency of Si at point Γ along the [111] direction as a test of accuracy of the recently developed full-potential linear muffin-tin orbitals method (FP-LMTO). By minimizing TE as a function of the phonon amplitude, excellent results, such as the equilibrium bond length and the phonon frequencies, were obtained. Also Tsai *et al.*¹⁹ have used the pseudofunction method to calculate the TE of cubic diamond Si as a function of Si—Si bond length.

In this work, we have used the self-consistent orthogonalized linear combination of atomic orbitals (OLCAO) method to calculate the electronic structures, total energies, and pressure-induced phase transformations of ten different forms of Si, including cubic diamond (cd), hexagonal diamond (hd), β -tin, simple hexagonal (sh), hexagonal close packed (hcp), face-centered cubic (fcc), two body-centered cubic phases, one with one atom per primitive cell (bcc) and the other with eight atoms per primitive cell B-8 ("bcc8"), simple cubic (sc), and a simple tetragonal with 12 atoms per unit cell T-12 ("st12"). In 1982, the same OLCAO method with slightly different computational procedures (to be discussed in Sec. II) was performed on cd-Si by Harmon *et al.*¹¹ They obtained excellent results in the structural and lattice dynamical properties of cd-Si. The motivation of the present work is to further demonstrate the accuracy of the OLCAO method in calculating the transition pressures (TP) and transition volumes (TV) for all possible phases of Si. Because of the small structural energy differences between some of the phases, these calculations require even higher accuracy than the earlier OLCAO TE calculations¹¹ which were applied to cd-Si only.

We will first discuss the method of calculation in Sec. II. In Sec. III we present our results which include TE and structural phase transitions of Si, band structures, density of states (DOS), and the charge densities of the ten phases of Si, lattice dynamics, and calculation of the internal strain parameter. In Sec. IV we summarize our results.

II. METHOD

In this work we have employed the SCF OLCAO method to calculate the electronic structures and TE of various phases of Si. Since the method has been described in detail elsewhere,¹² we limit our discussion to those aspects that are different from the earlier calculations.¹⁰⁻¹⁴ In the crystal calculation, the one-electron Schrödinger equation is solved within the LDF approximation. The basis functions are expressed in terms of 18 Bloch sums of the atomic orbitals of Si (1s, 2s, 2p, 3s, 3p, 3d, 4s, 4p). We have adopted the orthogonalization to the core procedure which makes the computations affordable. We have employed the self-consistent-field (SCF) Hartree-Fock-Slater method²⁰ to calculate the atomic wave functions, potentials, and charge densities for a radial grid of 250 mesh points which are expanded logarithmically from the nucleus for a maximum radius of 60.0 a.u. Then we searched for a set of Gaussian exponents (GE) α_i to least-squares fit the radial atomic wave functions $\Phi_{nl}(r)$ to a linear combination of Gaussian-type orbitals (GTO) of the form

$$\Phi_{nl}(r) = r^l \sum_{i=1}^{N_w} \phi_{ni} e^{-\alpha_i r^2} \quad (1)$$

where n and l are the principal and orbital quantum numbers, respectively, N_w is the number of the GTO's, and ϕ_{ni} are the coefficients to be obtained in the least-squares fitting procedure. We found that a set of 22 GTO's with exponents distributed geometrically from 0.1 to 10^9 would reproduce the calculated atomic wave functions with a root-mean-square (rms) fitting error of less than 0.001. A similar procedure has been engaged to find a set of GE β_i to least-squares fit the atomic potentials and charge densities to the forms

$$V(r) = -\frac{Z}{r} e^{-\beta_0 r^2} + \sum_{i=1}^{N_p} v_i e^{-\beta_i r^2} \quad (2)$$

and

$$\rho(r) = \sum_{i=1}^{N_p} \rho_i e^{-\beta_i r^2}, \quad (3)$$

respectively. In these equations, Z is the atomic number of Si, N_p is the number of the GTO's, and v_i 's and ρ_i 's are the coefficients to be obtained from the fit. We found that a set of 20 GTO's with GE's ranging from $\beta_{\min}=0.07$ to $\beta_{\max}=15000.0$ fits the potentials and charge densities with rms fit errors of less than 0.001 Ry and 1×10^{-5} electrons, respectively. This set has been obtained by slightly varying the middle term β_{mid} (the tenth term in this case) while following two geometrical distributions in the intervals $\beta_{\min} \rightarrow \beta_{\text{mid}}$ and $\beta_{\text{mid}} \rightarrow \beta_{\max}$ to get

the least rms fit error. In the present calculation, β_{mid} is calculated to be 12.0, which is also used as β_0 of the singular term of the total potential in Eq. (2).

In the crystal calculation, we have used the Wigner interpolation formula²¹ to calculate the exchange and correlation potentials. The major part of the input consists of the basic translational vectors of the crystal, atomic wave functions, and potentials in the form of linear combination of GTO's, the position of the basis atoms, a set of special \mathbf{k} points^{22,23} corresponding to the crystal symmetry, and a number of spacial directions used in generating a set of mesh points to be used in the treatment of the crystal exchange and correlation potentials. In the present work we have used a grid consisting of approximately 3500 mesh points which are radially distributed in 100 different directions about each basis atom. We have found that the convergence of the TE for the metallic phases of Si depends considerably upon the number of the mesh points, but is much less sensitive to the semiconducting phases of Si.

There are two outstanding differences in the present calculation and the earlier TE calculations performed by Harmon *et al.*¹¹ First, in the latter, in addition to the real atomic potential centers, some auxiliary sites were included within each unit cell. At each auxiliary site, they placed few single GTO's. The use of the auxiliary sites in their calculations resulted in an improvement in their SCF charge density. However, in the present calculations, we are considering ten different phases of Si for which there do not exist common locations for placing the auxiliary sites. Besides, we have tested the convergence of our calculated TE of the cd-Si against locating the auxiliary sites within the unit cells. By doing so, with the optimized set of the GE's, we did not observe any significant changes in our calculated TE. Therefore we chose not to use the auxiliary sites in our calculations. Second, Harmon *et al.* also scaled the radial extent of the GTO's of the wave functions, potentials, and the charge densities according to the size of the lattice parameter engaged in their TE calculations performed as a function of volume. In our calculation, we further tested the convergence of the total energies against the scaling of the radial extent of the GTO's. We found that, using this procedure with our optimized GE's, the total energy data points obtained could not be fitted to a polynomial or any other form of the equation of state (EOS) smoothly with a small rms fitting error. Besides, since our purpose has been to keep the GE parameters in the TE calculations of different phases the same, and because the scaling is paramount to a change of the original exponential parameters from one volume to another volume and from one phase to another phase, we have avoided using this scaling procedure in the present calculation.

The TE as a function of the volume has been calculated for the ten phases of Si using the same set of wave functions and potential GE discussed earlier in this section. We have used a larger number of special \mathbf{k} points for the metallic phases of Si so as to locate the Fermi levels more accurately and to achieve a better convergence. Careful tests of convergence of the TE against the number of the special \mathbf{k} points resulted in the requirement of using 10,

12, 8, 80, 144, 144, 60, 40, 120, and 6 special \mathbf{k} points in the irreducible region of the first BZ for the cd, hd, B-8, β -tin, sh, hcp, fcc, bcc, sc, and T-12 phases of Si, respectively. With this test, we have achieved a total energy convergence of approximately 0.001 Ry/atom for various phases of Si. We have also used the same optimized c/a ratios for the β -tin, sh, and hcp phases of Si as calculated by Liu, Chang, and Cohen² using PM. We utilized the experimental c/a ratios²⁴ for the other phases.

In each SCF iteration, the calculated charge densities are fitted by an unconstrained fit to the linear combination of GTO's as used for the potentials. The error of the total charge within a unit cell is then calculated with respect to the actual number of valence electrons in the unit cell. This error is an indication of the overall quality of the numerical fitting procedure. In the present calculation, we have achieved an error in the unconstrained fit of self-consistent charge density to less than $\pm 1 \times 10^{-5}$ electrons per unit cell. The iteration stops where the fitted potential stabilizes to less than 1×10^{-4} a.u.

For calculating the static structural properties of cd-Si, we have examined different forms of the EOS, such as the polynomial form of the TE, as a function of the lattice constant, the volume, and Murnaghan's EOS:²⁵

$$E_{\text{tot}}(V) = \frac{BV}{B'(B'-1)} \times \left[B' \left(1 - \frac{V_{\text{min}}}{V} \right) + \left(\frac{V_{\text{min}}}{V} \right)^{B'} - 1 \right] + E_{\text{min}}, \quad (4)$$

where V_{min} is the volume per atom corresponding to the minimum TE E_{min} , and B, B' are the bulk modulus and the pressure derivative of the bulk modulus at V_{min} , respectively. The variations in evaluating V_{min} and E_{min} in using different forms of the EOS were less than 0.01 \AA^3 and 0.001 Ry/atom , respectively. We have therefore used the polynomial form of the EOS to calculate V_{min} , E_{min} , TV, and TP because the linearity of the polynomial form of the EOS makes these calculations easier while retaining a reasonable accuracy. We have also made similar test calculations for B and B' . We obtained deviations up to 10% for B , and even larger variations for B' in using the polynomial form and the more accurate Murnaghan EOS. We have therefore used Murnaghan's equation to calculate B and B' , while using the calculated $E_{\text{min}}, V_{\text{min}}$ obtained from the polynomial form of the EOS.

For each crystal structure, we have calculated the TE at 6–20 different atomic volumes. The TE as a function of volume have been least-squares fitted to a polynomial of the order of 5–8. The rms errors of the fits were of the order of 0.0001 Ry/atom . The polynomial form of the EOS was then used to plot the total-energy curves.

The energy bands along the high-symmetry lines of the irreducible BZ, the DOS, and the charge densities have been calculated using the self-consistent potentials and charge densities thus obtained. We have utilized the Lehmann-Taut analytical linear tetrahedral method²⁶ with 240, 225, 196, 225, 225, 240, 140, 84, 140, and 126 \mathbf{k}

points in the irreducible portion of the BZ of cd, hd, β -tin, sh, hcp, fcc, bcc, sc, B-8, and T-12 phases, respectively, for an accurate evaluation of the DOS. This is especially important for precisely locating the Fermi levels of the metallic phases.

III. RESULTS

A. Total energy and phase transformation

The calculated TE as a function of volume for the ten phases of Si are shown in Fig. 1. The volumes are in the units of the experimental atomic volume V_{expt} of cd-Si. The crystal parameters and the number of the atoms in the unit cells used in our calculations, along with the number of the first nearest neighbors (NN) and their distances from the central atom, are listed in Table I. Also listed are the calculated V_{min} and E_{min} for each phase and the difference ΔE_{min} with respect to that of the cd-Si. From this table, we note that cd-Si has the lowest E_{min} , indicating that this is the most stable phase at the ambient pressure. The next smallest E_{min} belongs to hd-Si, the second most stable phase of Si. This is an expected result since these two phases have similar numbers of NN and distances over a long range. Moreover, we note that in an ascending order, B-8, β -tin, sh, sc, hcp, bcc, and fcc phases have higher ΔE_{min} , indicating the order of stability of the various phases. These results are in excellent agreement with those of the PM calculations.³

The static structural properties of cd-Si are obtained from the EOS in polynomial form and the Murnaghan's equation. We have used ten special \mathbf{k} points in an irreducible wedge of the BZ to calculate the TE at 20

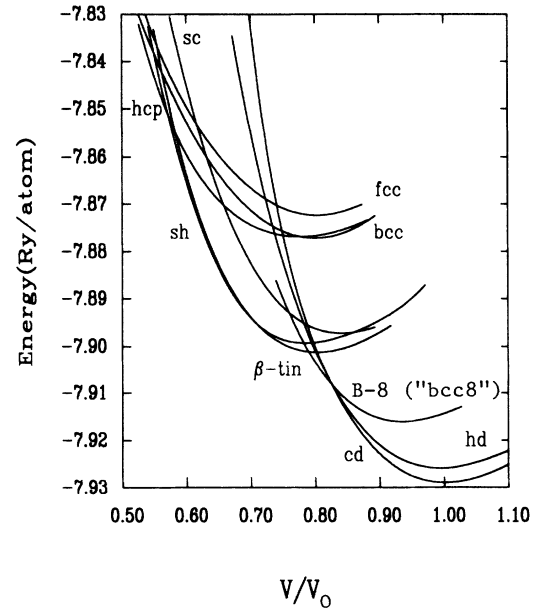


FIG. 1. Calculated total energy of various phases of Si as a function of volume. The volumes are in the units of the equilibrium volume per atom of cd-Si. Energies are in Ry/atom.

TABLE I. Crystal data of various phases of Si used in the present calculation and the resulting minimum total energies, equilibrium volumes, and the structural energy differences with respect to cd-Si. See text for explanation of data marked by an asterisk.

	cd	hd	β -tin	sh	sc	bcc	hcp	fcc	B-8	T-12
a (Å)	5.43	3.80	3.875	2.667	2.561	3.175	2.196	4.005	3.36	5.69
b (Å)	5.43	3.80	3.875	2.667	2.561	3.175	2.196	4.005	3.36	5.69
c (Å)	5.43	6.28	2.139	2.547	2.561	3.175	3.722	4.005	3.36	6.70
c/a	1.00	1.65	0.552	0.955	1.0	1.0	1.695	1.00	1.00	1.178
No. of atoms per unit cell	2	4	2	1	1	1	2	1	8	12
No. of NN	4	4	6	2	6	8	12	12	4	4
NN distance (Å)	2.350	2.35	2.487	2.547	2.561	2.749	2.196	2.832	2.37	2.39
V_{\min}/V_{expt}	1.00	0.994	0.803	0.784	0.840	0.800	0.777	0.803	0.935	0.904*
E_{\min} (Ry)	-7.9289	-7.9258	-7.9006	-7.8993	-7.8972	-7.8772	-7.8769	-7.8724	-7.916	-7.950*
ΔE_{\min} (eV)	0.0	0.042	0.385	0.403	0.431	0.703	0.707	0.768	0.175	-0.544*

different volumes ranging from $0.80V_{\text{expt}}$ to $1.12V_{\text{expt}}$. The calculated TE are then least-squares fitted to a polynomial of order 8 with a rms error of less than 1×10^{-5} Ry/atom. From the fit, we obtained an E_{\min} of -7.929 Ry/atom and an equilibrium lattice constant of 10.26 a.u. These results are to be compared with the experimental values of -7.92 Ry/atom (Ref. 27) and 10.26 a.u.²⁴ The calculated E_{\min} and V_{\min} , along with the 20 data points, were then least-squares fitted to the Murnaghan's equation to calculate B and B' . The rms of this fit is approximately 0.0001 Ry/atom and the B and B' values are 1.05 Mbar and 4.2 , respectively. These results are in excellent agreement with the experimental values²⁸ of 0.99 Mbar for B and 4.2 for B' . Harmon *et al.*,¹¹ using the same OLCAO method with different potential fitting parameters and slightly different procedures in preparing the atomic and crystal data, obtained -8.00 Ry/atom for E_{\min} , 10.40 a.u. for the lattice parameter, 0.89 Mbar for B , and 3.22 for B' . Yin *et al.*,⁶ using a first-principles PM, reported these quantities to be -7.91 Ry/atom for

E_{\min} , 10.30 a.u. for the lattice parameter, 0.98 Mbar for B , and 3.2 for B' . We have listed in Table II the results of the present work and those of Refs. 6, 11, and 19 with the corresponding percent deviations from the experimental values.

By applying pressure, cd-Si undergoes a series of structural phase transitions which have been observed experimentally.¹⁶⁻¹⁸ These are: cd \rightarrow β -tin, β -tin \rightarrow sh, sh \rightarrow hcp, and hcp \rightarrow fcc. The existence of hcp, fcc, sc, and bcc phases of Si were predicted by Yin *et al.*⁶ in their PM total-energy calculations. The other phases of Si, such as the hd-Si, B-8-Si, and T-12-Si are metastable phases of Si and are not induced by applying pressure to cd-Si. Experimentally, it has been shown that cd-Si transforms to β -tin Si at a pressure of 12 GPa.¹⁶⁻¹⁸ We can calculate this pressure based on the thermodynamics theorem that, when the transformation occurs, the Gibbs free energy

$$G = E_{\text{tot}} + PV - TS \quad (5)$$

TABLE II. Comparison of the equilibrium lattice constant a_{\min} , minimum total energy E_{\min} , bulk modulus B , and the pressure derivative of the bulk modulus B' calculated by the present work, earlier OLCAO calculations (Ref. 11), pseudopotential calculations (Ref. 6), pseudofunction (Ref. 19), and the experimental results. Percent deviations from the measured values are given adjacent to the calculated values.

	a_{\min} (a.u.)	E_{\min} (Ry/atom)	B (Mbar)	B'
Present calc.	10.26(0%)	$-7.929(0.1\%)$	$1.05(6\%)$	$4.2(0\%)$
Ref. 11	$10.40(1.4\%)$	$-8.003(1\%)$	$0.89(10\%)$	$3.22(23\%)$
Ref. 6	$10.30(0.4\%)$	$-7.91(-0.1\%)$	$0.98(1\%)$	$3.2(23\%)$
Ref. 19	$10.21(-0.5\%)$	$-7.82(-1.2\%)$	$1.03(4\%)$	$3.4(19\%)$
Expt.	10.26^a	-7.92^b	0.99^c	4.2^c

^a Reference 24.

^b Reference 27.

^c Reference 28.

becomes equal between the two phases. At zero temperature, which is considered in these calculations, the transformation occurs along the common tangent between the TE curves of the two phases. The negative of the slope of the tangent gives the TP.

We have calculated the TE of β -tin Si at several different volumes using the optimized c/a ratio of 0.551 of Ref. 4. Since β -tin Si is a metallic phase of Si, a larger number of special k points (80) in the BZ than that used for the cd-Si is required. This is expected, since the TE depends on the accurate determination of the Fermi level. Our calculated TE for cd-Si and β -tin Si along with their common tangent is shown in Fig. 2(a). Our calculation gives a TP of 15.4 GPa, which is in reasonable agreement with the experimental values of about 12 GPa. It also

shows that cd-Si undergoes this transition at a volume of $0.89V_{\text{expt}}$ to β -tin at $0.71V_{\text{expt}}$. These values have been measured^{16,17} to be $0.91V_{\text{expt}}$ and $0.71V_{\text{expt}}$ for the cd-Si and β -tin Si, respectively. Liu *et al.*² calculated this transition to occur at 9.9 GPa, with the TV of $0.931V_{\text{expt}}$ for cd-Si and $0.719V_{\text{expt}}$ for β -tin Si.

In 1984, it was reported by Hu *et al.*¹⁶ and Olijnyk *et al.*¹⁷ that β -tin Si transforms into an intermediate sh phase before transforming to a hcp structure. This phase was not considered in the PM total-energy calculation of Yin and Cohen⁶ for the β -tin \rightarrow hcp phase transformation. The pressure for this transformation has been measured to be ranging from 13.2 to 16.4 GPa. We have calculated the TE of the sh phase as a function of volume using the optimized c/a ratio of 0.995 as suggested by

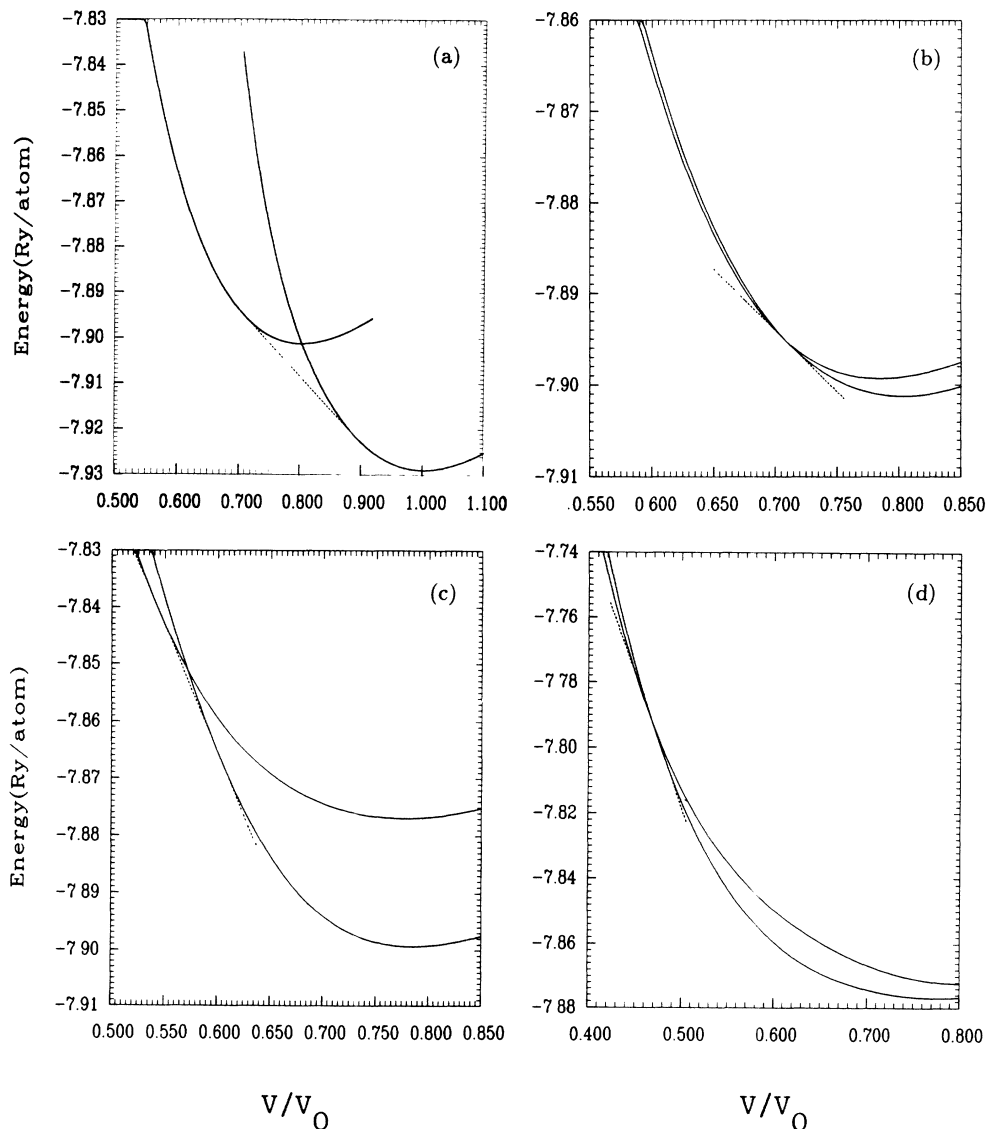


FIG. 2. Calculated total energy and structural phase transition for (a) cd-Si \rightarrow β -tin Si, (b) β -tin Si \rightarrow sh-Si, (c) sh-Si \rightarrow hcp-Si, (d) hcp-Si \rightarrow fcc-Si.

Ref. 2, using 144 special \mathbf{k} points. The TE of β -tin Si and sh-Si as a function of their atomic volume and their common tangent are shown in Fig. 2(b). Our calculated TP for β -tin to sh-Si is 15.3 GPa, which is in the range of the reported experimental values. This transition occurs at a volume of $0.71V_{\text{expt}}$ for β -tin Si and $0.69V_{\text{expt}}$ for sh-Si, which compare very well with experimental values^{16,17} of $0.69V_{\text{expt}}$ for the β -tin and $0.67V_{\text{expt}}$ for sh-Si. The PM calculation of Ref. 2 obtained a TP of 12.0 GPa, and a TV of $0.707V_{\text{expt}}$ for β -tin and $0.69V_{\text{expt}}$ for the sh phase.

The sh-Si, in turn, transforms into the hcp phase at about 40 GPa as measured experimentally.^{16,17} We have used 144 special \mathbf{k} points for the TE calculation of this phase using the optimized c/a ratio of 1.695 as suggested by Ref. 3. The TE for the sh-Si and the hcp-Si phases along with their common tangent are shown in Fig. 2(c). Our calculation shows that this transition occurs at the pressure of 46 GPa. This is also in good agreement with the experimentally measured value, and the result of the PM calculation³ which reported a TP of 41 GPa. The calculated TV for sh-Si is $0.594V_{\text{expt}}$, and that of hcp-Si is $0.547V_{\text{expt}}$. These quantities are to be compared with the experimental values of $0.615V_{\text{expt}}$ for the sh-Si and $0.570V_{\text{expt}}$ for the hcp-Si and the PM values² of $0.603V_{\text{expt}}$ and $0.556V_{\text{expt}}$, respectively.

The fcc-Si is induced by applying a pressure of 78 GPa (Ref. 18) to hcp-Si. This is a free-electron-like phase of Si with a metallic band structure (see Sec. III B 6). We have used 60 special \mathbf{k} points for the TE calculation of this phase. Figure 2(d) shows the calculated TE of hcp-Si, fcc-Si, and their common tangent. Our calculation gives a TP of 89 GPa with TV of $0.477V_{\text{expt}}$ for hcp-Si, and $0.460V_{\text{expt}}$ for fcc-Si. These are to be compared with the measured values¹⁸ of $0.481V_{\text{expt}}$ for the hcp-Si and $0.475V_{\text{expt}}$ for the fcc-Si, respectively, with a TP of 78 GPa. Chang *et al.*,³ using the PM, have calculated the TP to be 116 GPa, much larger than the experimental value, and TV of $0.465V_{\text{expt}}$ and $0.456V_{\text{expt}}$ for the hcp and fcc phases, respectively. Also, our calculated B of the fcc-Si is close to that of the cd-Si, while the PM obtained a B value for the fcc-Si phase over 5 times larger than that of the cd-Si. It is possible that at such a high pressure, core states start to play a significant part in the overall electronic structure, and the PM description becomes less accurate. Moriarty and McMahan²⁹ calculated a TP of 76 GPa using the LMTO method and obtained the TV of hcp-Si to be $0.496V_{\text{expt}}$. By using the generalized pseudopotential theory²⁹ (GPT), the same authors were able to improve their results for the TP and TV to 80 GPa and $0.482V_{\text{expt}}$, respectively.

The existence of the bcc and sc phases of Si was also first predicted by Yin and Cohen.^{5,6} We have used 80 special \mathbf{k} points for the TE calculation of the bcc-Si phase. Our TE are slightly lower than those of the hcp phase at volumes larger than $0.78V_{\text{expt}}$. The PM gave similar results.³ Their TE of the bcc-Si are also smaller than those of the hcp-Si starting at volumes larger than $0.80V_{\text{expt}}$. McMahan and Moriarty³⁰ predicted the phase transformation from fcc-Si to bcc-Si to be in the pressure range of 250–360 GPa. However, this transition

has not yet been verified experimentally. Our TE calculations are up to pressures of the hcp \rightarrow fcc phase transformation, which is far below the pressures in the possible fcc \rightarrow bcc transition. Our calculated TE for sc-Si using 120 special \mathbf{k} points are lower than the hcp phase over a wide range of volumes down to $0.65V_{\text{expt}}$, suggesting that sc-Si is more stable than the hcp-Si phase. Chang and Cohen³ have obtained similar results for the TE of the sc-Si with respect to those of the hcp phase.

hd-Si has a wurtzite structure and is a semiconducting phase of Si, so that 12 special \mathbf{k} points would be sufficient for the TE calculation. The TE of this phase have been calculated using the experimental²⁴ c/a ratio of 1.653. Our calculated EV of $0.99V_{\text{expt}}$ is in excellent agreement with the measured value²⁴ of $0.98V_{\text{expt}}$. Our calculated TE at the EV is only 0.042 eV higher than that of the cd-Si. This phase is not a pressure-induced phase of Si, since its transition Gibbs free energy is higher than that of the β -tin phase. Similar results have been obtained by Yin *et al.*,⁶ although they obtained an even smaller energy difference between this phase and the cd-Si phase.

We have further calculated the TE of the metastable B-8 phase,³¹ a body-centered-cubic phase with eight atoms in the primitive cell. The common tangent of the TE curve of this phase with that of the cd-Si also gives a higher Gibbs free energy than that of cd-Si to β -tin Si. Nevertheless, this phase can be formed as pressure is released from the β -tin Si.³¹ Our calculated EV of B-8-Si is $0.935V_{\text{expt}}$ per atom, which is in good agreement with the experimental result³¹ of $0.912V_{\text{expt}}$. The PM (Ref. 32) gave a TV of $0.903V_{\text{expt}}$.

Unlike the T-12-Ge, which has been identified as a high-pressure phase of germanium,³³ the T-12-Si has not been observed experimentally. The T-12 structure is commonly used as a model structure for calculating the electronic structure of amorphous Si (Refs. 7, 34, and 35) because of the presence of five-member rings. To explore the possibility of this phase theoretically, we have calculated its TE at several different atomic volumes with the internal parameters³³ equal to those of T-12-Ge. We have used a c/a ratio as suggested by Joannopoulos and Cohen.⁷ The calculated TE were not giving a minimum over a wide range of volumes. This result may suggest that Si does not exist in the T-12 phase as Ge does. R. Biswas *et al.*³² have calculated the TE of T-12-Si for one point which is higher than that of the B-8-Si and lower than the β -tin Si by relaxing its structural parameters. They concluded that T-12-Si can be a stable phase of Si. Their relaxed parameters and the c/a ratio were not given. However, the existence of a stable T-12 phase for Si with other c/a ratios and optimal crystal parameters cannot be ruled out at this time.

We have summarized the results of the present calculation of the TP and volumes of pressure-induced phase transformations of Si in Table III. Also listed are the corresponding experimental values and the results from other theoretical calculations.

B. Electronic structures

In this section, we present the result of our SCF band-structure calculations, the corresponding DOS, and the

TABLE III. Transition volumes V_t and pressures p_t of various phases of Si calculated by the present work, other theoretical calculations, and the measured values.

Transition	$V_t(\text{cd})$	$V_t(\beta\text{-tin})$	$V_t(\text{sh})$	$V_t(\text{hcp})$	$V_t(\text{fcc})$	p_t (GPa)
$\text{cd} \rightarrow \beta\text{-tin}$						
Present calc.	0.89	0.71				15.4
Other calc.	0.931 ^a	0.719 ^a				9.9 ^a
	0.915 ^b	0.707 ^b				9.5 ^b
	0.928 ^c	0.718 ^c				9.9 ^c
	0.926 ^d	0.719 ^d				10.0 ^d
Experiment	0.918 ^e	0.710 ^e				12.5 ^f
	0.911 ^g	0.706 ^g				11.3 ^g
	0.92 ^h					
$\beta\text{-tin} \rightarrow \text{sh}$						
Present calc.		0.71	0.69			15.3
Other calc.		0.707 ^a	0.692 ^a			12.0 ^a
		0.678 ^c	0.661 ⁱ			14.3 ⁱ
		0.683 ^b	0.672 ^b			14.9 ^b
		0.69 ^h	0.673 ^g			16.0 ^h
Experiment						13.2–16.4 ^g
$\text{sh} \rightarrow \text{hcp}$						
Present calc.			0.594	0.547		46.0
Other calc.			0.603 ^a	0.556 ^a		41.0 ^a
			0.580 ^b	0.538 ^b		
		0.608 ^d		0.563 ^d		41.0 ^d
Experiment			0.615 ^g	0.570 ^g		35.0–40.0 ^h
				0.54 ^g		36.0–42.0 ^g
$\text{hcp} \rightarrow \text{fcc}$						
Present calc.				0.477	0.460	88.0
Other calc.				0.465 ^a	0.456 ^a	116.0 ^a
				0.482 ^d		80.0 ^d
Experiment				0.481 ^j	0.475 ^j	78.0 ^j

^a Reference 3.

^b Reference 36.

^c Reference 5.

^d Reference 30.

^e Reference 37.

^f References 38 and 39.

^g References 16 and 40.

^h Reference 17.

ⁱ Reference 41.

^j Reference 18.

TABLE IV. Comparison of energy eigenvalues of cd-Si (in units of eV) at Γ , L , and X calculated by the present work, other theoretical calculations, and the measured values.

	Present work	EMTO (Ref. 48)	Pseudopotential (Ref. 5)	LAPW (Ref. 8)	Pseudofunction (Ref. 19)	Experiment
Γ_1	-12.18	-11.87	-11.93	-12.02	-12.52	-12.4±0.6 ^a
$L_{2'}$	-9.63	-9.69	-9.52	-9.64	-9.77	-9.3±0.4 ^a
L_1	-7.1	-6.98	-7.00	-7.06	-7.23	-6.4±0.4 ^a
Σ_1	-4.4		-4.52			-4.7±0.2 ^{a,b}
					-4.4 ^c	
X_4	-3.05	-2.92	-2.88	-2.82	-2.98	-2.5±0.3 ^b
$L_{3'}$	-1.41	-1.27	-1.20	-1.16	-1.38	-1.2±0.2 ^c

^a Reference 45.

^b Reference 44.

^c Reference 47.

valence-charge densities (VCD) in the plane containing a Si—Si bond for the ten phases of Si. In Table I we have listed the crystal data used in our calculations.

1. *cd-Si*

The calculated band structure of *cd-Si* at the experimental EV (Ref. 24) along the symmetry lines of the irreducible $\frac{1}{48}$ BZ of the fcc lattice is shown in Fig. 3(a). The top of the valence band (TVB) is at $0.81\Gamma X$ along the axis from $\Gamma \rightarrow X$, which is in excellent agreement with the experimental value⁴² of 0.82. Our indirect band gap is 0.76 eV, which is 35% lower than the experimental value of 1.17 eV. This reduction in band gap is consistent with the generally accepted notion that the LDF which was developed for the ground-state properties underestimates the gap. Recently several theoretical methods have been developed to improve the gap value by applying the many-body corrections to the local-density approximation,⁴³ but we have not used them in this work. Yin and Cohen⁵ have obtained a band gap of 0.55 eV using the first-principles PM.

The calculated DOS using the analytic linear tetrahedral method²⁶ using 240 k points in the irreducible part of the BZ is displayed in Fig. 4(a). The peak positions are in excellent agreement with those of the experimentally determined values from the angle-integrated photoemission spectra,^{44–47} and those of the PM calcula-

tions.⁵ In Table IV we compare the eigenvalues corresponding to the peak positions in the DOS at Γ , X , and L with the measured values and with other theoretical results. The difference of our eigenvalues at these points with those of the PM is approximately 0.37 eV for Γ , and much smaller for others.

The VCD of *cd-Si* at the experimental volume, has been calculated in the (110) plane. The contour plot in this plane is shown in Fig. 5(a). It is noted that there is a large maximum charge along the bond indicating a strong covalent bond in the *cd-Si*. Our calculated VCD is in good agreement with the experimental results⁴⁹ determined by the x-ray diffraction for the same plane. Our calculated VCD is also in excellent agreement with that of Weyrich⁹ using full-potential LMTO method, and that of Yin and Cohen⁵ using the PM.

2. *hd-Si*

This phase contains four atoms per unit cell with a wurtzite structure.²⁴ The NN are tetrahedrally bonded with bond lengths almost the same as the *cd-Si*. The major structural difference of the two phases is that *hd-Si* has four extra neighbors at 3.90 Å in addition to the 12 second-nearest neighbors at 3.83 Å. Its EV per atom is $0.99V_{\text{expt}}$. The equilibrium TE of the two phases are very close, with that of the *cd* phase being 0.042 eV lower. We

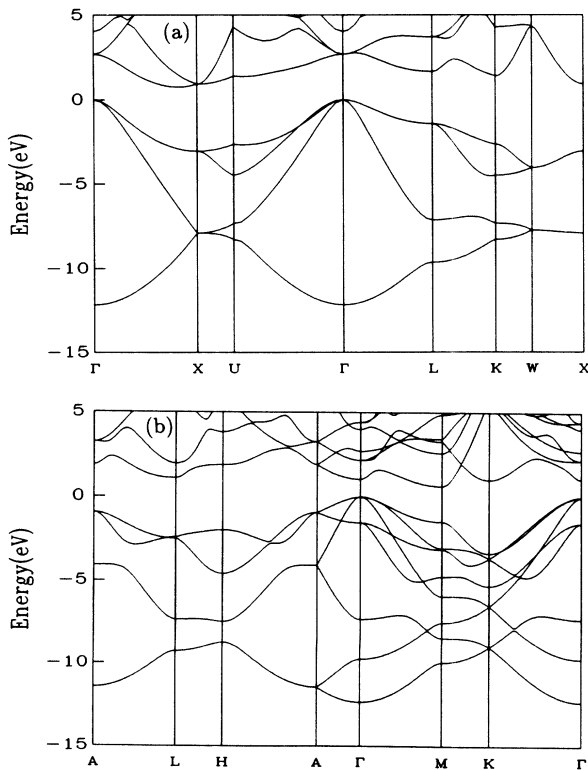


FIG. 3. Calculated band structure of (a) *cd-Si*, (b) *hd-Si*. Energies are measured from the top of the VB.

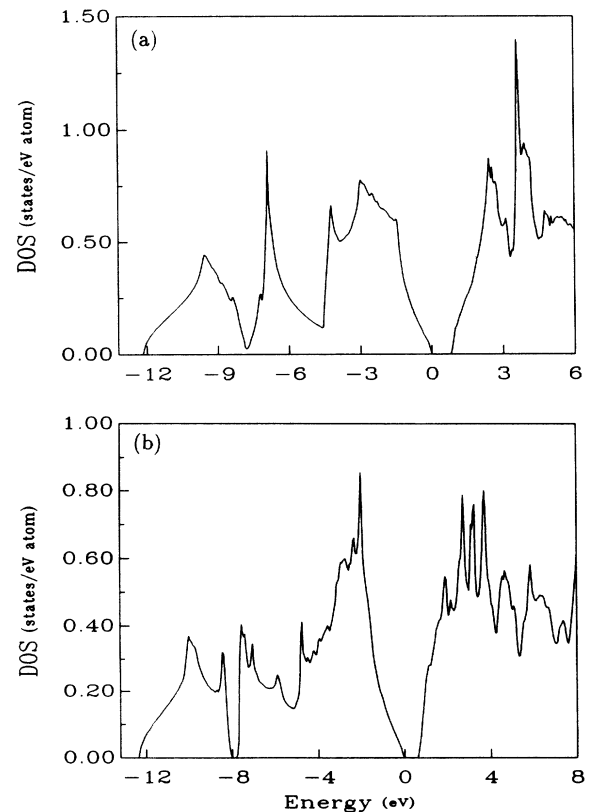


FIG. 4. Calculated DOS of (a) *cd-Si*, (b) *hd-Si* in units of states/eV atom.

may expect that the hd phase having electronic properties the same as the cd-Si. The result of our band-structure calculation for hd-Si is shown in Fig. 3(b). We have obtained an indirect band gap of 0.6 eV, with the TVB to be at Γ and the bottom of the conduction band (BCB) at M . Using a semi-*ab initio* OLCAO method, Huang and Ching⁵⁰ have calculated the electronic structure of this phase using a minimal basis function. They obtained a very similar band structure and DOS, and a direct band gap of 1.067 eV located at Γ . However, in the semi-*ab initio* approach of Huang and Ching, the exchange potential was adjusted so as to give the experimental gap value of 1.17 eV for cd-Si. In comparison, the present results are also in good agreement with the empirical-pseudopotential (EMP) calculations of Joannopoulos and Cohen.⁷ They obtained an indirect band gap of 0.85 eV with the TVB at Γ and the BCB at M .

The calculated DOS of hd-Si is shown in Fig. 4(b). It shows peak positions similar to those of the cd phase. The widths of the valence band in both phases are slightly larger than 12 eV.

The calculated VCD in the $(\bar{2}110)$ plane is shown in Fig. 5(b). It is practically the same as those of the cd-Si in the (110) plane, as expected.

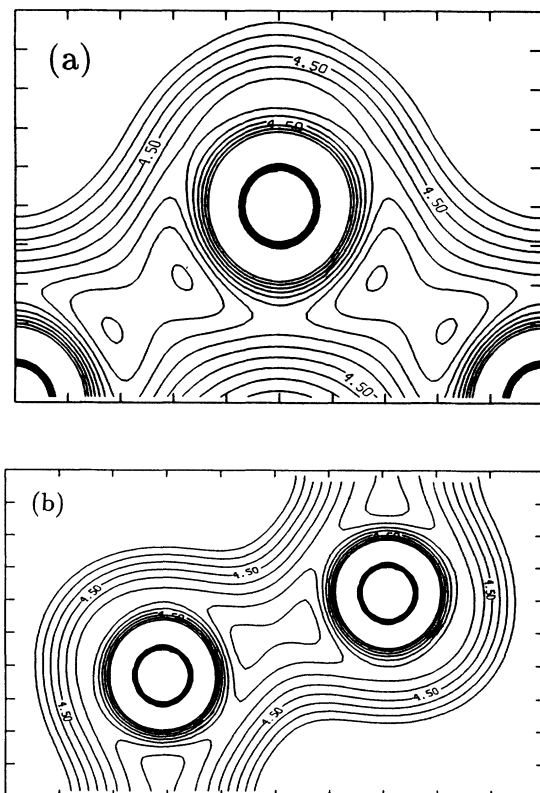


FIG. 5. Contour plot of the calculated VCD of (a) cd-Si in the (110) plane, (b) hd-Si in the $(\bar{2}110)$ plane. The units are in electrons per unit cell. The contours have equal intervals of 0.005 electrons. The contour values have been scaled by 100.

3. β -tin Si

The band structure and DOS of β -tin Si at the volume of $V_{\min} = 0.803V_{\text{expt}}$ are shown in Figs. 6(a) and 7(a), respectively. The results characterize this phase to be metallic, in agreement with experiment.^{51,37} We have used 196 k points at the corners of 648 tetrahedra for an accurate determination of the position of the Fermi level which lies at about 10.31 eV above the BVB. The contour plots of our calculated VCD in the (100) plane is displayed in Fig. 8(a). From this figure, it is noted that there still exists a considerable amount of covalent bonding in spite of a metallic band, although the charge distri-

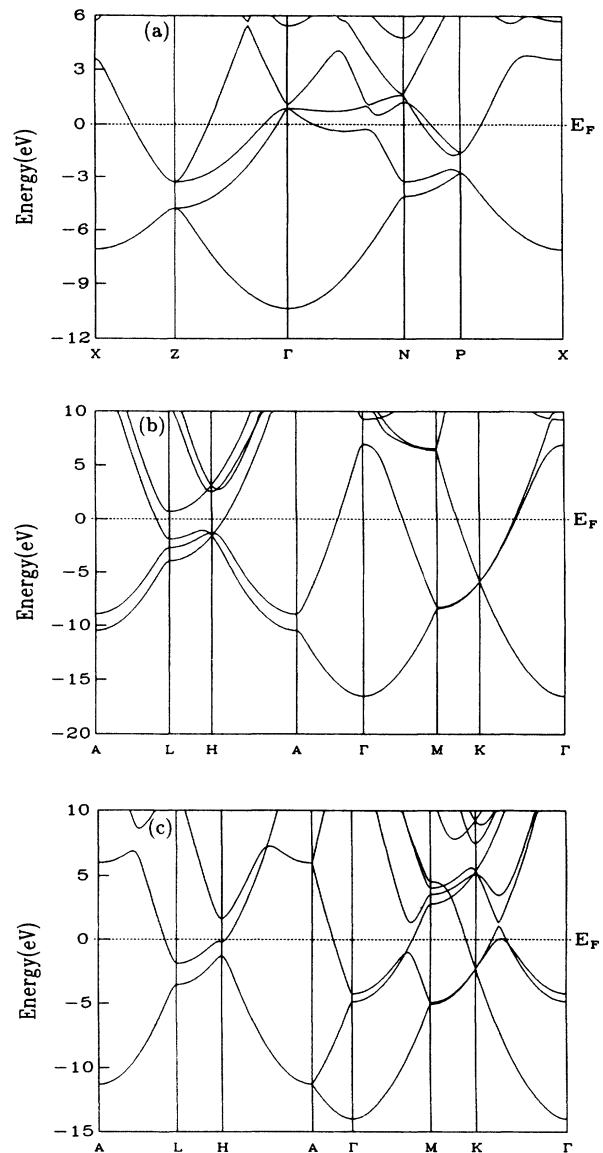


FIG. 6. Calculated band structure of (a) β -tin Si at the equilibrium volume with the experimental c/a of 0.552, (b) sh-Si at the transition volume of 20.0 \AA^3 per atom and the optimized c/a of 0.955, (c) hcp-Si at the transition volume of 9.54 \AA^3 per atom and the optimized c/a of 1.695.

bution is quite different from the cd-Si. The PM (Ref. 5) gave similar results for the electronic properties of this phase.

4. *sh-Si*

We have calculated the electronic band structure, DOS, and VCD of *sh-Si* at a volume of $12.6 \text{ \AA}^3/\text{atom}$. At the vicinity of this volume, Si transforms to the hcp phase. Our results are to be compared with those of the PM calculation of Chang and Cohen⁴ performed at the same atomic volume and the same optimized c/a ratio of 0.955. Our results for the band structure, DOS, and VCD contour are shown in Figs. 6(b), 7(b), and 8(b), re-

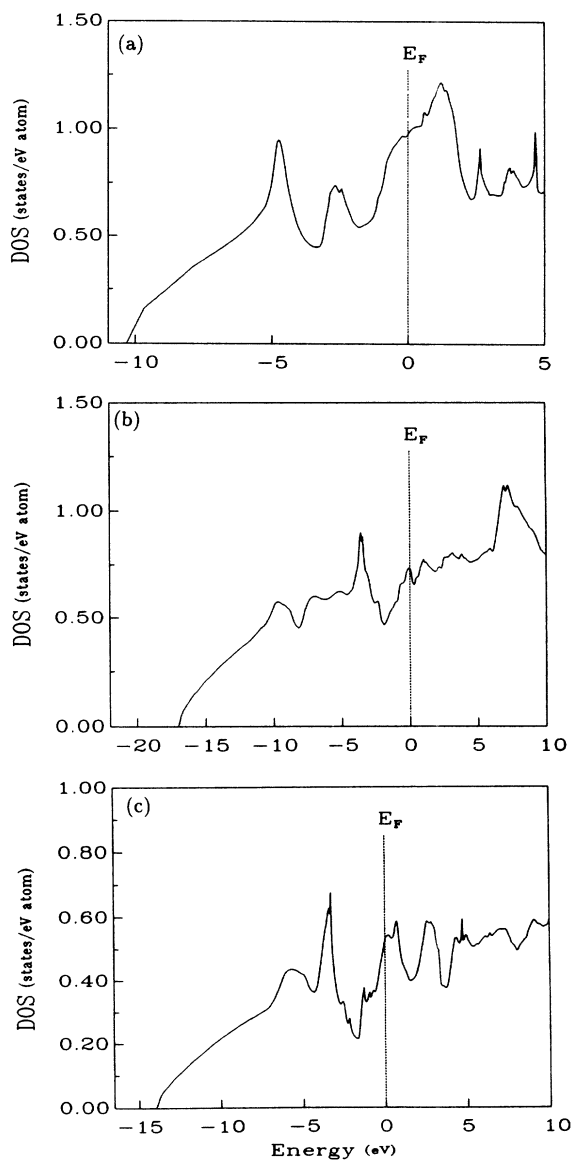


FIG. 7. Calculated DOS of (a) β -tin Si, (b) *sh-Si*, (c) hcp-Si in units of states/eV atom.

spectively. These results are in excellent agreement with those of the PM calculation. The DOS was calculated using 255 \mathbf{k} points at the corners of 768 tetrahedra. The Fermi level is found to be at 16.5 eV above the BVB, which compared to the 16.0 eV obtained in Ref. 4.

The contour plot of the VCD in the $(10\bar{1}0)$ plane shown in Fig. 8(b) shows a strong covalent bond along the c axis and a minimum local charge along the a axis. These results are also in good agreement with those of Ref. 4.

5. *hcp-Si*

The calculated band structure, DOS, and VCD of the hcp-Si at its transition volume ($0.48V_{\text{expt}}$) to fcc structure, using a c/a ratio of 1.695, are shown in Figs. 6(c), 7(c), and 8(c), respectively. We have used 225 \mathbf{k} points or 768 tetrahedra in the evaluation of DOS. The band and DOS characterize hcp-Si to be a metallic phase of Si with a Fermi level which lies at 14.43 eV above the BVB. The contour plot of VCD at the $(11\bar{2}0)$ plane is shown in Fig. 8(c). The bond charge of this phase is weaker than that of the *sh-Si*, which indicates a more metallic characteristic of this phase. The VCD of hcp-Si has also been calculated by the PM in the same plane but at a different volume of $0.75V_{\text{expt}}$.⁵

6. *fcc-Si*

The electronic band and DOS of the fcc-Si calculated at the TV of $0.46V_{\text{expt}}$ are shown in Figs. 9(a) and 10(a), respectively. In this calculation, we have used 240 \mathbf{k} points (or 864 tetrahedra) and obtained a Fermi level at 20.0 eV above the BVB, which is in excellent agreement with 19.45 eV calculated by the PM (Ref. 2) at slightly smaller volume. The DOS near the BVB shown in Fig. 10(a) is closely proportional to $E^{1/2}$, indicating a free-electron-like phase for fcc-Si at this volume.

The contour plots of the VCD in the (100) plane are shown in Fig. 11(a). They are in good agreement with that of the PM.⁴ Even in this metallic phase, there is still some charge buildup between the Si—Si bond.

7. *sc-Si*

For the *sc* phase, we have calculated the band structure and DOS at the calculated EV of $V_{\text{min}} = 0.84V_{\text{expt}}$. Eigenvalues at 84 \mathbf{k} points (216 tetrahedra) have been used to locate the Fermi level accurately. The results of our calculations are shown in Figs. 9(b) and 10(b), which indicate that *sc-Si* is also metallic. The calculated Fermi level lies at 18.24 eV above the BVB.

The contour plot of the VCD in the (100) plane is shown in Fig. 11(b), which is in good agreement with the PM calculations⁵ performed at a slightly different volume of $0.75V_{\text{expt}}$. Their charge buildup between the Si—Si bond is much weaker than that in the fcc-Si phase of Fig. 11(a). However, it is difficult to make such comparisons because their calculations were carried out at different volumes.

TABLE V. Calculated Fermi level, DOS (states/eV atom) at the Fermi level (metallic phases), TVB, band gap (semiconducting phases), and the corresponding atomic volume for various phases of silicon. Fermi level and the TVB are measured with respect to the bottom of the valence band. Volumes are in units of the equilibrium volume of the cubic diamond phase (V_{expt}).

Si phase	Volume (V_{expt})	Fermi level (eV)	TVB (eV)	Gap (eV)	DOS (states/eV atom)
cd	1.00		12.184	0.76	
hd	0.994		12.396	0.60	
B-8	0.935		13.00	-0.37	
β -tin	0.803	10.31			0.98
sh	0.594	16.496			0.731
hcp	0.477	14.432			0.527
fcc	0.460	20.0			0.571
sc	0.840	18.242			0.350
bcc	0.800	16.648			0.427
T-12	0.904		12.5	1.6	

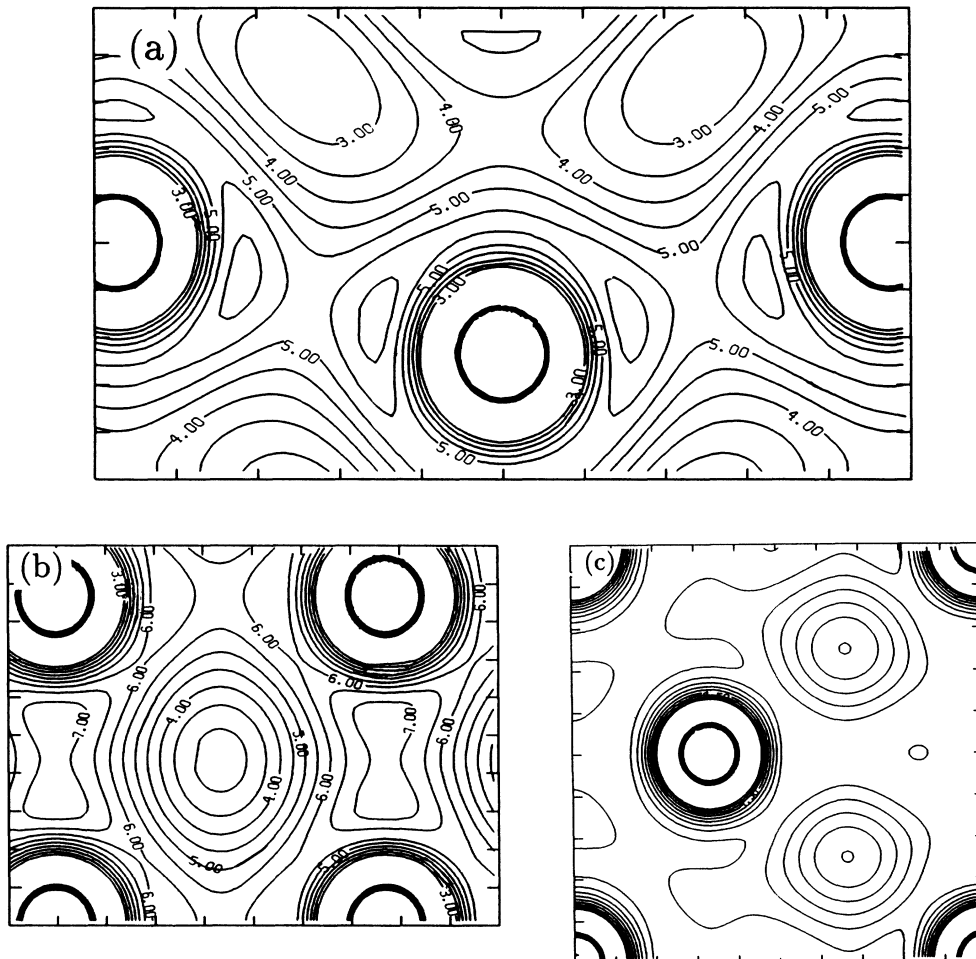


FIG. 8. Contour plot of the calculated VCD of (a) β -tin Si in the (100) plane, (b) sh-Si in the (0 $\bar{1}$ 0) plane, (c) hcp-Si in the (11 $\bar{2}$ 0) plane in units of electrons per unit cell (the contours intervals are the same as Fig. 5).

8. bcc-Si

The band structure, DOS, and the VCD of the bcc-Si are calculated at its EV $V_{\min} = 0.80V_{\text{expt}}$. The DOS has been calculated using 140 k points (432 tetrahedrons). The results are shown in Figs. 9(c), 10(c), and 11(c), respectively. It shows bcc-Si to be metallic with the Fermi level at 16.65 eV above the BVB. The calculated VCD in the (100) plane is shown in Fig. 11(c), which is in good agreement with those of the PM of Yin and Cohen,⁵ which has been performed at the volume of $0.75V_{\text{expt}}$.

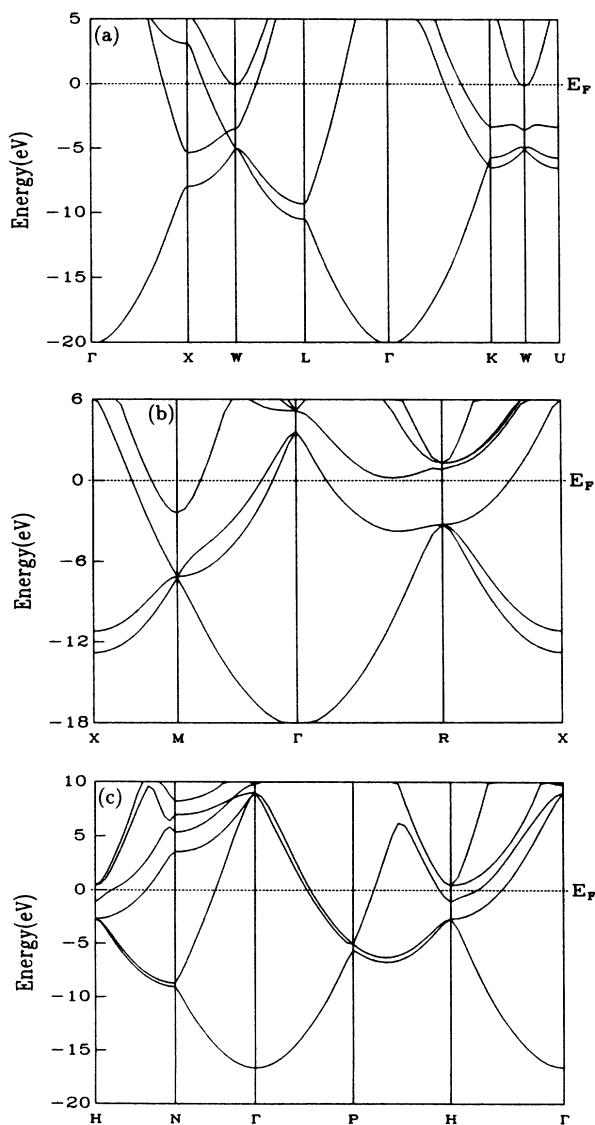


FIG. 9. Calculated band structure of (a) fcc-Si at the transition volume of 9.20 \AA^3 per atom, (b) sc-Si, (c) bcc-Si at the volume corresponding to the minimum of the total-energy curves. Energies are measured from the Fermi level (dashed lines).

9. B-8-Si

The band structure of B-8-Si is shown in Fig. 12(a). In this structure we have found a band overlap of about 0.3 eV at H , characterizing this phase to be a semimetal. This is in agreement with the earlier *ab initio* non-SCF OLCAO calculations of Ching and Lin.³⁴ Similar results have been obtained by the EMP calculations,⁷ except they found a direct band gap of 0.43 eV at H . Our calculated DOS for the B-8-Si using the tetrahedral method with 140 k points at the corners of 432 tetrahedrons is shown in Fig. 13(a). We have calculated the Fermi level to be at 12.5 eV above the bottom of the valence band (BVB).

The contour plot of the calculated VCD in the (110) plane is shown in Fig. 14(a). The charge distribution along the Si-Si bond is very similar to the cd-Si, and we conclude that strong covalent bonding is retained in this phase.

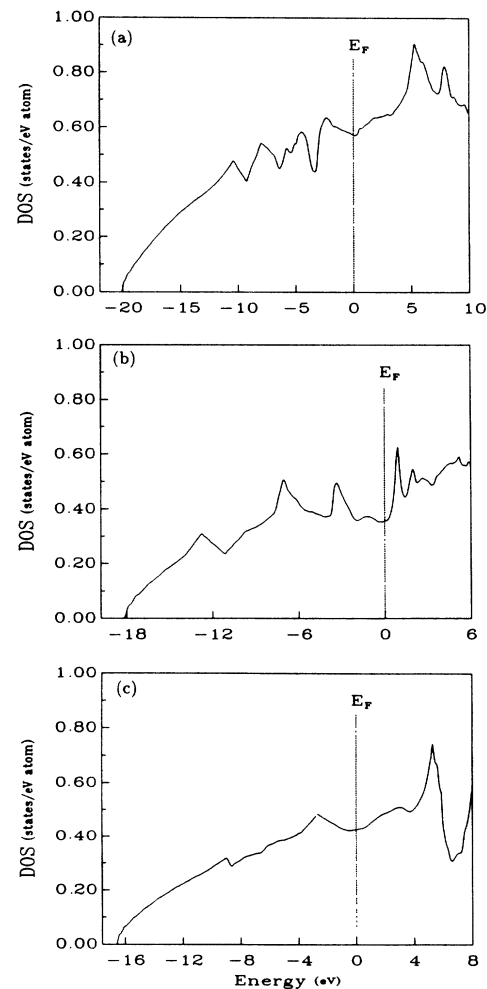


FIG. 10. Calculated DOS of (a) fcc-Si, (b) sc-Si, (c) bcc-Si in units of states/eV atom.

10. T-12-Si

The results of the band structure and DOS for the T-12 structure are shown in Figs. 12(b) and 13(b), respectively. We have obtained a semiconducting band structure with an indirect band gap of 1.6 eV. The TVB is at Γ and the BCB is at Z. Our results are in excellent agreement with those of the PM (Ref. 52) and the earlier non-SCF OLCAO results.³⁵ Since T-12-Si may not exist, this result can only be considered as existing for a particular model structure of Si.

In Table V, we summarize the results of electronic

structures for the ten different phases of Si. These include the atomic volumes, width of the VB, gap size for the semiconducting phases, and DOS at the Fermi level for the metallic phases.

C. Lattice dynamics

In this section, we present the result of our calculation of the phonon frequencies of cd-Si (Refs. 53–66) at Γ and X. We adopt the Born-Oppenheimer approximation,⁶⁶ which assumes that the electrons are in the ground state

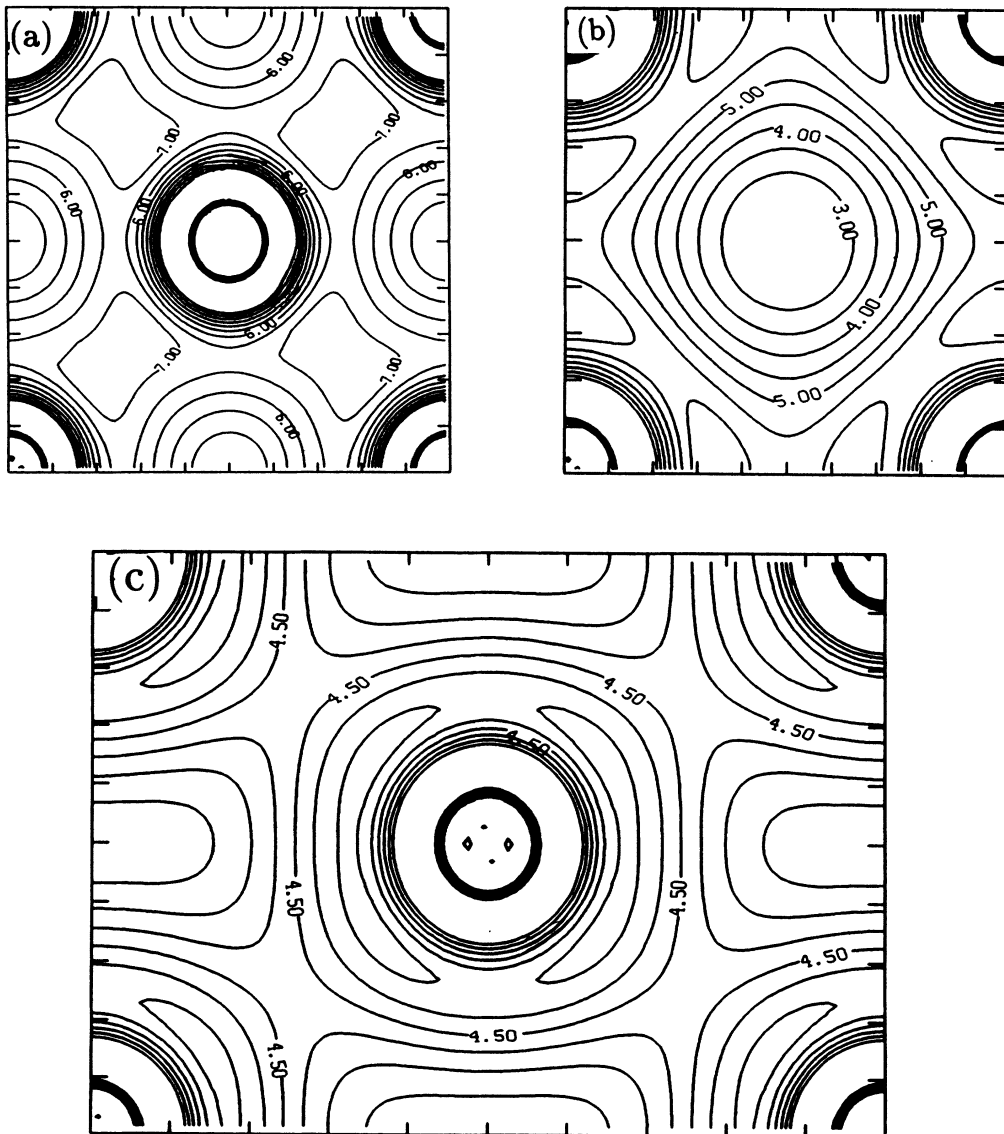


FIG. 11. Contour plot of the calculated VCD of (a) fcc-Si in the (100) plane, (b) sc-Si in the (100) plane, (c) bcc-Si in the (110) plane in units of electrons per unit cell (the contour intervals are the same as Fig. 5).

with respect to the instantaneous nuclear position. The same atomic wave function and potential fitting function as utilized for the TE and phase-transformation calculations of the undistorted cd-Si are used for consistency. Within the harmonic approximation, the force constants of these modes are obtained from the second derivative of the TE (per atom) with respect to the phonon amplitude u :

$$k = \left. \frac{\partial^2 E_{\text{tot}}}{\partial u^2} \right|_{u=0} \quad (6)$$

Then the phonon frequency is given by

$$f = \frac{\sqrt{k/M}}{2\pi}, \quad (7)$$

where M is the atomic mass. The distorted primitive cell for phonon calculations at Γ contains two atoms per unit cell with trigonal symmetry (D_{3d}). By symmetry, the LO(Γ) and TO(Γ) modes are degenerate, and we refer to these modes as LTO(Γ). We have used 14 special k points in the $\frac{1}{12}$ of the BZ of the trigonal lattice. The TE have been calculated as a function of the phonon amplitude for a displacement range of $\pm 0.1 \text{ \AA}$ along the [111]

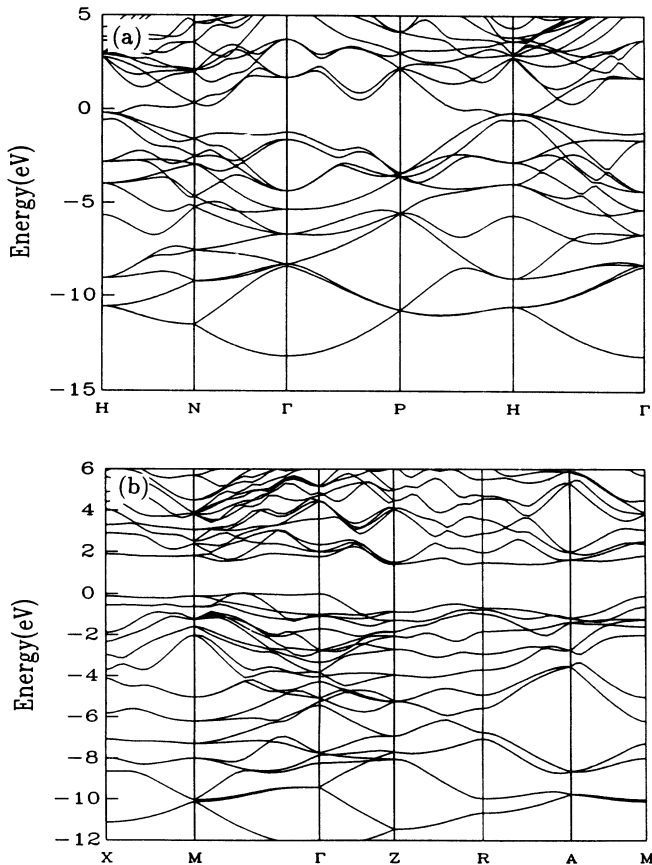


FIG. 12. Calculated band structure of (a) B-8-Si, (b) T-12-Si. Energies are measured from the top of the VB.

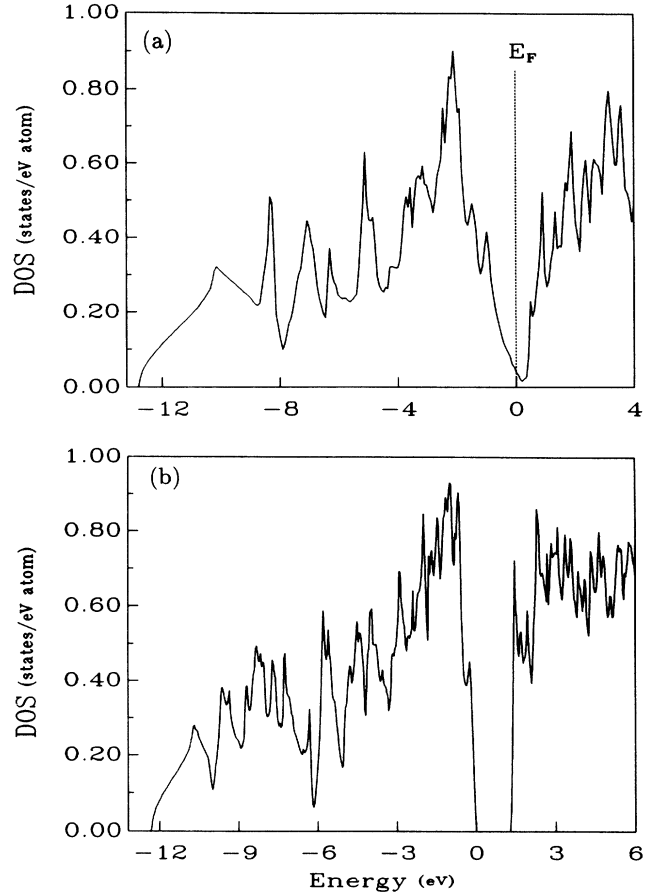


FIG. 13. Calculated DOS of (a) B-8-Si, (b) T-12-Si in units of states/eV atom.

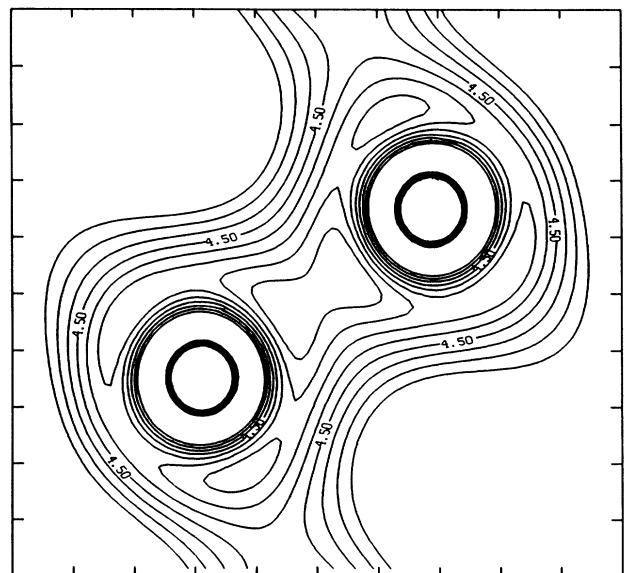


FIG. 14. Contour plot of the calculated VCD of the B-8-Si in the (110) plane. The units are in electrons per unit cell (the contour intervals are the same as Fig. 5).

direction. The resulting TE are fitted to a polynomial of the order 6 with a rms fit error of 2.6×10^{-5} Ry/atom, which is shown in Fig. 15(a). As can be seen from this figure, the anharmonicity of this mode increases with an increase in phonon amplitude. We have calculated the phonon frequency using the second derivative of the fitted polynomial at the equilibrium atomic positions, $u=0$. Our calculated phonon frequency for LTO(Γ) is 15.35 THz, which is in very good agreement with the experimental value of 15.53 THz.

We have also calculated the average force constant using the TE differences^{5,55} ΔE with respect to the equilibrium TE by the following approximation:

$$k \simeq \frac{\Delta E}{\frac{1}{2}u^2}. \quad (8)$$

In this way, we obtained a phonon frequency of 15.10 THz, which is close to that obtained by using the second derivative of the fitted polynomial curve. Harmon *et al.*,¹¹ using the same OLCAO method with somewhat different optimized Gaussian parameters, calculated the frequency of this mode to be 15.0 THz. Yin and Cohen⁵ obtained an average frequency of 15.15 THz by using the PM and Eq. (8).

We have further calculated the cubic force constant

k_{xyz} corresponding to the third-order anharmonic term of this mode^{5,55} using the equation

$$\Delta E(u) = \frac{1}{2}ku^2 + 4k_{xyz} \left[\frac{u}{\sqrt{3}} \right]^3. \quad (9)$$

We obtained $k_{xyz} = -30.1 \text{ eV/\AA}^3$, which compares favorably with the experimental value of -35.1 eV/\AA^3 . The experimental value was obtained from utilizing the measured values of the third-order force constants⁶⁵ in conjunction with the Keating model involving anharmonic force constants.⁶¹ References 11 and 5 gave the k_{xyz} values of -34.3 and -32.7 eV/\AA^3 , respectively which are in better agreement with the experimental value.

For a calculation of the phonon frequency of Si at the edge of the BZ, the size of the primitive cell must be doubled. We have used a tetragonal primitive cell with four basis atoms in the TE calculation for the TA(X) phonon mode. We used eight special \mathbf{k} points in $\frac{1}{16}$ of the BZ. For this mode, the TE were calculated for several different phonon amplitudes ranging from 0.0 to $\pm 0.05 \text{ \AA}$ and fitted to a polynomial of the order 5. The rms error of the fit was better than 10^{-5} Ry/atom. The result of our calculation is shown in Fig. 15(b). Our calculated phonon frequency is 4.65 THz, which can be compared with the measured value^{57,58} of 4.49 THz. The theoretical phonon frequency of this mode using the PM (Ref. 6) is 4.45 THz, while Harmon *et al.*¹¹ obtained a frequency of 4.9 THz using the OLCAO method.

The results of our lattice dynamic calculation, together with the measured frequencies and other existing theoretical values, are summarized in Table VI. It is fair to say that our calculation for phonon frequency in Si is of comparable accuracy to the other state-of-the-art calculations.

D. Internal strain parameter

In this section we present the result of our calculations of the internal strain parameter ξ (Refs. 67–74) for cd-Si along the [111] direction by minimizing the TE as a function of ξ . In this calculation, a trigonal unit cell with two atoms per unit cell was used. The atomic positions of Si in the trigonal crystal under stress are given by⁶⁷

$$\mathbf{R}'_1 = (\mathbf{I} + \underline{\varepsilon})\mathbf{R}_1, \quad (10)$$

$$\mathbf{R}'_2 = (\mathbf{I} + \underline{\varepsilon})\mathbf{R}_2 - \frac{1}{2}a\xi\varepsilon_2 \begin{pmatrix} 1 \\ 1 \\ 1 \end{pmatrix}, \quad (11)$$

TABLE VI. Comparison of the phonon frequencies of the cd-Si at Γ and X calculated by the present work, other theoretical calculations, and the experimental values.

	LTO(Γ) phonon (THz)	k_{xyz} (eV/\AA^3)	TA(X) (THz)
Present calc.	15.35	-30.1	4.65
Ref. 11	15.0	-34.3	4.90
Ref. 5	15.15	-32.7	4.45
Expt.	15.53	-35.1	4.49

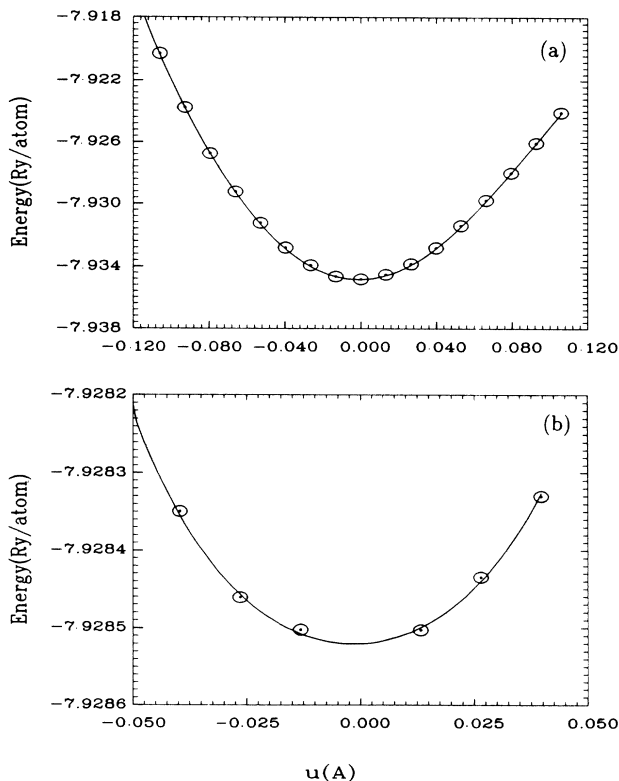


FIG. 15. (a) Total energy of the cd-Si as a function of the phonon amplitude along the [111] direction for the LTO(Γ) mode. (b) Total energy of cd-Si as a function of the phonon amplitude for the TA(X) mode.

where \mathbf{R}_1 and \mathbf{R}_2 are the positions of the atoms in the unstrained unit cell, a is the cubic diamond lattice parameter, ξ is the internal strain parameter, and $\underline{\varepsilon}$ is the uniaxial stress tensor in the [111] direction of the form

$$\underline{\varepsilon} = \begin{pmatrix} \varepsilon_1 & \varepsilon_2 & \varepsilon_2 \\ \varepsilon_2 & \varepsilon_1 & \varepsilon_2 \\ \varepsilon_2 & \varepsilon_2 & \varepsilon_1 \end{pmatrix}, \quad (12)$$

where ε_1 and ε_2 define a pure hydrostatic volume change and a pure trigonal deformation, respectively. For every set of ε_1 and ε_2 , we have calculated the TE for seven different values of ξ between 0.1 and 1.0. Fourteen special \mathbf{k} points in the irreducible $\frac{1}{12}$ of the BZ have been used, and the TE converged to better than 1×10^{-5} Ry/atom. The TE data are then fitted to a polynomial of the order of 4 and the internal strain parameter is obtained from the minimum position of the TE versus ξ curve.

We have performed the calculations for four different sets of $\varepsilon_1, \varepsilon_2$:

- (i) $\varepsilon_1 = 0.0, \varepsilon_2 = -0.02$,
- (ii) $\varepsilon_1 = 0.0, \varepsilon_2 = -0.035$,
- (iii) $\varepsilon_1 = 0.0, \varepsilon_2 = -0.04$,
- (iv) $\varepsilon_1 = \varepsilon_2 = \frac{1}{3}(0.04)$.

In the first three cases, the volume change vanishes as a result of a 4%, 7%, and 8% compression in the [111] direction, and a 2%, 3.5%, and 4% expansion in the (111) plane, respectively. In each case the TE are fitted to a polynomial of the order 4 with a rms fitting error of about 4×10^{-5} Ry/atom. The minimum of the three cases occurred at $\xi = 0.40$, $\xi = 0.50$, and $\xi = 0.64$, respectively.

In the case (iv), the volume is increased by 4% as a result of a 4% bond stretching in the [111] direction, whereas the distances in the (111) planes do not change. In this case, we obtained no minimum but a kink at $\xi = 0.73$. In spite of the reasonable accuracy of our TE calculations, we obtained different values of ξ for different cases, depending on how the crystal is set under stress. J. Sanchez-Dehesa *et al.*,⁶⁷ using the PM, have also obtained different values of ξ for different ways of stressing the crystal. They obtained $\xi_i = 0.816$, $\xi_{ii} = 0.785$, and $\xi_{iii} = 0.99$ for the three cases of (i) $\varepsilon_1 = \varepsilon_2 = -0.02$, (ii) $\varepsilon_1 = \varepsilon_2 = -\frac{1}{3}(0.04)$, and (iii) $\varepsilon_1 = \varepsilon_2 = \frac{1}{3}(0.04)$, respectively. Harmon *et al.*¹¹ had obtained $\xi = 0.61$ using a similar OLCAO method by applying a strain of $\sim 4.7\%$ along the [111] direction. Weber⁷⁴ used the adiabatic bond-charge model (ABCM) for cd-Si and obtained ξ to be 0.5. The experimental values of ξ have been reported to be 0.6 (Ref. 72) and 0.73.⁷³ The average of our four calculations gives a value of 0.57 for ξ which is low compared to the experimental values. However, as mentioned above, theoretical calculation of ξ is not unique. Rather, it depends on the assumption made with regards to the crystal distortion. Similarly, the analysis of experimental data may not be unique and subject to additional corrections. With this in mind, we consider our calculated values for the internal strain param-

eter to be quite reasonable.

The result of this and other theoretical calculations, together with the measured values, are summarized in Table VI.

IV. SUMMARY AND CONCLUSIONS

In the present work, we have successfully demonstrated the accuracy of the OLCAO method within the local-density approximation by calculating the static structural properties of various phases of Si, such as the equilibrium volume, bulk modulus, the pressure derivative of the bulk modulus, the transition pressures and volumes, and the electronic states, as well as some dynamical properties of the cd-Si phase. In summary we have obtained the following results:

(i) We have calculated the static structural properties of the cd-Si from first principles by calculating the TE as a function of the crystal volume. We have obtained the equilibrium lattice parameter to be 10.26 a.u. The bulk modulus to be 1.05 Mbar, and the pressure derivative of the bulk modulus to be 4.2, which are in very good agreement with experiments. Our calculated B is 6% larger than the measured value of 0.99 Mbar. This value can probably be improved by further optimizing the fitting Gaussian parameters for crystal charge density. We have obtained a band gap of 0.76 eV, which is 35% smaller than the measured value.

(ii) We have further tested the accuracy of our method in predicting the phase transitions of Si under high pressures up to 100 GPa, and calculated the TV and TP for various phases of Si. Our calculated TV's are at most 5% different from the average of the measured values. TP's are more difficult to obtain both experimentally and by calculation. Up to 30% difference in TP has been cited in the reported measured values. We have up to a 24% deviation with respect to the average of different experimental values. Our results are also in quite good agreement with the first-principles pseudopotential calculations. At very high pressures, we have obtained a TP of 89 GPa for hcp-Si to fcc-Si, which compares very well with the experimental value of 80 GPa.

(iii) The electronic band structures, the DOS, and the VCD of the ten different phases of Si calculated in the present work are presented. They are generally in very good agreement with the measured values and the results of the pseudopotential calculations.

(iv) For lattice dynamics in the cd phase, we have obtained a frequency of 15.35 THz for the LTO(Γ) mode, with 1% deviation from the measured value, and a frequency of 4.65 THz for the TA(X) mode, compared to the measured value 4.45 THz.

(v) Moreover, we have calculated the internal strain parameter ξ in the [111] direction of the cd-Si, which varies between 0.4 and 0.73 depending on the way the crystal is set under stress. Our results are in reasonable agreement with the measured values of 0.6 and 0.73 and the results of other theoretical calculations (see Table VII).

Our extensive calculation of ground-state properties of various phases of Si using the local-density approximation demonstrates that the OLCAO method is capable of

TABLE VII. Comparison of the internal strain parameter ξ calculated by the present work, other theoretical calculations, and the experimental values.

	Internal parameter ξ
Present calc.	0.4, 0.553, 0.645, 0.730
Ref. 11	0.61
Ref. 67	0.86
Ref. 74	0.50
Expt.	0.62, 0.73

giving accurate total-energy results comparable to those of the first-principles pseudopotential method. The accuracy of the OLCAO calculation can probably be further improved if optimized fitting parameters for the potential and charge-density functions can be obtained. At this time, there appears to be no simple and efficient way of determining the optimal set of fitting parameters, and more developmental work in this regard is warranted.

However, one advantage of the OLCAO method is its economic use of the basis function and its versatility in application to different types of condensed matter systems, and, as such, the OLCAO method will have a great advantage in studying the energetics of complex systems within the local-density approximation. With further development of the method to improve its accuracy and efficiency, it may eventually be possible to tackle problems such as phase transitions and defect migrations in complex ceramic oxides and nitrides.

ACKNOWLEDGMENTS

One of the authors (F.Z.) would like to thank Dr. K. J. Chang and A. M. Liu, who collaborated on the pseudopotential calculations at the University of California, Berkeley for their helpful discussions. This work is supported by the U.S. Department of Energy Grant No. DE-FG02-84ER45170.

- ¹W. Kohn and L. J. Sham, *Phys. Rev.* **140**, A1133 (1965).
²A. Y. Liu, K. J. Chang, and M. L. Cohen, *Phys. Rev. B* **37**, 6344 (1987).
³K. J. Chang and M. L. Cohen, *Phys. Rev. B* **31**, 7819 (1985).
⁴K. J. Chang and M. L. Cohen, *Phys. Rev. B* **30**, 5376 (1984).
⁵M. T. Yin and M. L. Cohen, *Phys. Rev. B* **26**, 5668 (1982).
⁶M. T. Yin and M. L. Cohen, *Phys. Rev. B* **45**, 1004 (1980).
⁷J. D. Joannopoulos and M. L. Cohen, *Phys. Rev. B* **7**, 2644 (1972).
⁸D. R. Hamann, *Phys. Rev. Lett.* **42**, 662 (1979).
⁹K. H. Weyrich, *Phys. Rev. B* **37**, 10269 (1988).
¹⁰W. Y. Ching and B. N. Harmon, *Phys. Rev. B* **34**, 5305 (1986).
¹¹B. N. Harmon, W. Weber, and D. R. Hamann, *Phys. Rev. B* **25**, 1109 (1982).
¹²J. A. Appelbaum and D. R. Hamann, in *Transition Metals*, edited by M. J. G. Lee, J. M. Perz, and E. Fawcett (IOP, Bristol, 1980), p. 111.
¹³P. J. Feibelmann, J. A. Appelbaum, and D. R. Hamann, *Phys. Rev. B* **20**, 1433 (1979).
¹⁴J. A. Appelbaum and D. R. Hamann, *Solid State Commun.* **27**, 881 (1978).
¹⁵J. R. Chelikowsky and S. G. Louie, *Phys. Rev. B* **29**, 3470 (1983).
¹⁶Z. Hu and I. L. Spain, *Solid State Commun.* **51**, 263 (1984).
¹⁷H. Olijnyk, S. K. Sikka, and W. B. Holzapfel, *Phys. Lett.* **103A**, 137 (1984).
¹⁸S. J. Duclos, Y. K. Vohra, and A. L. Ruoff, *Phys. Rev. Lett.* **58**, 775 (1987).
¹⁹M.-H. Tsai, J. D. Dow, and R. V. Kasowski, *Phys. Rev. B* **38**, 2176 (1988).
²⁰J. P. Desclaux, *Comp. Phys. Commun.* **1**, 216 (1969).
²¹E. Wigner, *Phys. Rev.* **46**, 1002 (1934).
²²H. J. Monkhorst and J. D. Pack, *Phys. Rev. B* **13**, 5189 (1976).
²³D. J. Chadi and M. L. Cohen, *Phys. Rev. B* **8**, 5747 (1973).
²⁴J. Donohue, *The Structures of the Elements* (Wiley, New York, 1974).
²⁵F. D. Murnaghan, *Proc. Nat. Acad. Sci. USA* **30**, 244 (1944).
²⁶G. Lehmann and M. Taut, *Phys. Status Solidi B* **54**, 469 (1972).
²⁷L. Brewer, Lawrence Berkeley Laboratory Report No. LB-3720, May 1977 revision (for the cohesive energy at 0 K) (unpublished); C. E. Moore, *Atomic Energy Levels*, Nat. Bur. Stand. (U.S.) Circular No. 467 (U.S. GPO, Washington, D.C., 1949), Vol. 1.
²⁸H. J. Mc Skimin, *J. Appl. Phys.* **24**, 988 (1953).
²⁹J. A. Moriarty and A. K. McMahan, *Phys. Rev. Lett.* **48**, 809 (1982).
³⁰A. K. McMahan and J. A. Moriarty, *Phys. Rev. B* **27**, 3235 (1983).
³¹R. H. Wentorf, Jr. and J. S. Kasper, *Science* **139**, 338 (1963).
³²R. Biswas, R. M. Martin, R. J. Needs, and O. H. Nielsen, *Phys. Rev. B* **30**, 3210 (1984).
³³J. S. Kasper and S. M. Richards, *Acta Crystallogr.* **17**, 752 (1964).
³⁴W. Y. Ching and C. C. Lin, *Phys. Rev. B* **12**, 5536 (1975).
³⁵W. Y. Ching and C. C. Lin, *Phys. Rev. B* **16**, 2989 (1977).
³⁶M. T. Yin, in *Proceedings of the 17th International Conference on the Physics of Semiconductors*, San Francisco, 1984 (unpublished), as cited in Ref. 3.
³⁷J. C. Jamieson, *Science* **139**, 762 (1963); **139**, 845 (1963).
³⁸G. J. Piermarini and S. Block, *Rev. Sci. Instrum.* **46**, 973 (1975).
³⁹W. A. Weinstein and G. J. Piermarini, *Phys. Rev. B* **12**, 1172 (1975).
⁴⁰C. S. Mononi, J. Z. Hu, and I. L. Spain, *Phys. Rev. B* (to be published).
⁴¹R. Needs and Martin, *Phys. Rev. B* **30**, 5390 (1984).
⁴²K. L. Shalee and R. E. Nahony, *Phys. Rev. Lett.* **24**, 942 (1970).
⁴³W. Kohn, *Phys. Rev. B* **33**, 4331 (1986).
⁴⁴L. Ley, S. Kowalczyk, R. Pollak, and D. A. Shirley, *Phys. Rev. Lett.* **29**, 1088 (1972).
⁴⁵W. D. Grobman and D. E. Eastman, *Phys. Rev. Lett.* **29**, 1508 (1972).
⁴⁶W. D. Grobman, D. E. Eastman, and J. L. Freeouf, *Phys. Rev. B* **12**, 405 (1975).
⁴⁷W. E. Spicer and R. Eden, in *Proceedings of the Ninth International Conference on the Physics of Semiconductors*, 1968 (Nauka, Leningrad, 1968), Vol. 1, p. 61, as cited in Ref. 5.
⁴⁸M. S. Hybertson and S. G. Louie, *Phys. Rev. Lett.* **55**, 1418

- (1985).
- ⁴⁹M. A. Spackman, *Acta Crystallogr. Sect. A* **42**, 271 (1986).
- ⁵⁰M. Z. Huang and W. Y. Ching, *Solid State Commun.* **47**, 89 (1983).
- ⁵¹M. C. Gupta and A. L. Ruoff, *J. Appl. Phys.* **51**, 1072 (1980).
- ⁵²M. L. Cohen and J. R. Chelikowsky, *Solid State Sci.* **75** (1988).
- ⁵³K. Maschke and A. Baldereschi, in *Physics of Semiconductors 1978*, edited by B. L. H. Wilson (IOP, Bristol, 1979), p. 673.
- ⁵⁴M. Born and K. Huang, *Dynamical Theory of Crystal Lattices* (Oxford University Press, New York, 1954), Chap. V.
- ⁵⁵K. Kunc and R. M. Martin, in *Ab initio Calculation of Phonon Spectra*, edited by J. T. Devreese, V. E. Van Doren, and P. E. Van Camp (Plenum, New York, 1983), pp. 49–99.
- ⁵⁶G. Dolling, *Inelastic Scattering of Neutrons in Solids and Liquids* (IAEA, Vienna, 1963), Vol. II, p. 37.
- ⁵⁷G. Dolling, *Inelastic Scattering of Neutrons in Solids and Liquids* (IAEA, Vienna, 1963), Vol. II, p. 249.
- ⁵⁸G. Nilson and G. Nelin, *Phys. Rev. B* **6**, 3777 (1972).
- ⁵⁹G. Nilson and G. Nelin, *Phys. Rev. B* **3**, 364 (1971).
- ⁶⁰J. Ihm and M. L. Cohen, *Solid State Commun.* **37**, 491 (1981).
- ⁶¹P. N. Keating, *Phys. Rev.* **149**, 674 (1966).
- ⁶²P. N. Keating, *Phys. Rev.* **145**, 637 (1966).
- ⁶³P. N. Keating, *Phys. Rev.* **140**, A369 (1965).
- ⁶⁴H. J. McSkimin, P. Andreatch, Jr., and R. N. Thurston, *J. Appl. Phys.* **36**, 1624 (1965).
- ⁶⁵H. J. McSkimin and P. Andreatch, Jr., *J. Appl. Phys.* **35**, 3312 (1965).
- ⁶⁶M. Born and J. R. Oppenheimer, *Am. J. Phys.* **84**, 451 (1927).
- ⁶⁷J. Sanchez-Dehesa, C. Tejedor, and J. A. Verges, *Phys. Rev. B* **26**, 5960 (1982).
- ⁶⁸J. Sanchez-Dehesa, J. A. Verges, and C. Tejedor, *Phys. Rev. B* **24**, 1006 (1981).
- ⁶⁹L. Kleinman, *Phys. Rev.* **128**, 2614 (1962).
- ⁷⁰C. S. G. Cousins, *J. Phys. C* **15**, 1857 (1982).
- ⁷¹C. S. G. Cousins, L. Gerward, J. Staun Olsen, B. Selsmark, and B. J. Sheldon, *Acta Crystallogr. Sect. B* (to be published), as cited in Ref. 67.
- ⁷²A. Segmuller and H. R. Neyer, *Phys. Kondens. Mater.* **4**, 63 (1965).
- ⁷³H. d'Amour, W. Denner, H. Schulz, and M. Cardona, *Acta Crystallogr. Sect. B* (to be published), as cited in Ref. 67.
- ⁷⁴W. Weber, *Phys. Rev. B* **15**, 4789 (1977).